



Published in final edited form as:

J Thromb Thrombolysis. 2020 July ; 50(1): 98–111. doi:10.1007/s11239-020-02112-9.

AKT2 regulates endothelial-mediated coagulation homeostasis and promotes intrathrombotic recanalization and thrombus resolution in a mouse model of venous thrombosis

Wanmu Xie^{1,2}, Lin Zhang^{1,3}, Wei Luo^{1,3}, Zhenguo Zhai^{4,5}, Chen Wang^{2,4,5}, Ying H. Shen^{1,3}

¹Division of Cardiothoracic Surgery, Michael E. DeBakey Department of Surgery, Baylor College of Medicine, One Baylor Plaza, BCM 390, Houston, TX 77030, USA

²National Clinical Research Center for Respiratory Diseases, Beijing, China

³Texas Heart Institute, Houston, TX, USA

⁴Department of Respiratory and Critical Care Medicine, China-Japan Friendship Hospital, 2 Yinghua Dongjie, Hepingli, Beijing 100029, China

⁵Department of Respiratory Medicine, Capital Medical University, Beijing, China

Abstract

Venous thromboembolism (VTE) carries a high risk of morbidity and mortality. Understanding the mechanisms of venous thrombus formation and resolution is critical for improving VTE management. AKT2 kinase is essential for platelet activation and arterial thrombosis. In this study, we examined the role of AKT2 in venous thrombosis in a mouse model of venous thrombosis induced by inferior vena cava (IVC) ligation. We observed an induction of AKT2 expression in the ligated IVC of wild-type (WT) mice. Interestingly, although the initial thrombus size of the ligated IVC was similar between *Akt2*^{-/-} mice and WT mice, thrombus resolution was delayed in the ligated IVC of *Akt2*^{-/-} mice. Compared with the ligated IVC of WT mice, the ligated IVC of *Akt2*^{-/-} mice displayed decreased levels of thrombomodulin (TM) and increased levels of tissue factor (TF), apoptosis, and necroptosis. In addition, intrathrombotic endothelial cells in the ligated IVC of *Akt2*^{-/-} mice failed to form small vessels, resulting in impaired recanalization and thrombus resolution. TGF- β signaling activation and fibrotic remodeling were increased in the thrombus and vein wall of the ligated IVC of *Akt2*^{-/-} mice. We further investigated the AKT2-mediated regulation of coagulation factors in endothelial cells and found that forkhead box protein O1 (FOXO1), a target of AKT, enhanced TF and inhibited TM expression. By inhibiting FOXO1, AKT2 suppressed TF expression while increasing TM expression. Our findings indicate that AKT2 may protect endothelial cells against cell death, regulate endothelial-mediated coagulation homeostasis, and promote intrathrombotic recanalization and thrombus resolution in venous

Chen Wang: cyh- birm@263.net, Ying H. Shen: hyshe@bcm.edu.

Author Contributions W.X., L.Z., W.L., Z.Z., C.W., and Y.H.S. designed the studies. W.X., L.Z., and W.L. performed the experiments. W.X., L.Z., W.L., Z.Z., and Y.H.S. analyzed the data. W.X., C.W., and Y.H.S. wrote the manuscript, which was revised by all authors.

Conflict of interest All authors declare that they have no conflict of interest.

Compliance with Ethical Standards

Publisher's Note Springer Nature remains neutral with regard to jurisdictional claims in published maps and institutional affiliations.

thrombosis. These observations suggest dynamic roles of AKT2 in venous thrombus formation and resolution.

Keywords

AKT; FOXO1; Tissue factor; Thrombomodulin; Venous thrombosis

Introduction

Venous thromboembolism (VTE), including deep vein thrombosis (DVT) and pulmonary thromboembolism, carries a high risk of morbidity and mortality [1–4]. Despite significant improvements made in the prevention and treatment of VTE in recent years, many patients are still affected by recurrent DVT, post thrombotic syndrome [4, 5], recurrent pulmonary embolism [4], and chronic thromboembolic pulmonary hypertension [4, 6]. Understanding the mechanisms of venous thrombus formation and resolution is critical for improving VTE management.

Various risk factors trigger venous thrombosis by altering blood flow, activating endothelial cells, and inducing inflammation that lead to increased coagulation. Once a thrombus has formed, thrombus resolution resembles the wound healing process: inflammatory cells are recruited to the thrombus and clear the damaged tissues, and matrix metalloproteinases are produced to break down matrix [7–12]. Intrathrombotic recanalization is essential for thrombus resolution [13, 14]. Venous thrombus formation and resolution are dynamic processes that involve the delicate control of multiple pathways in various types of cells.

The serine/threonine kinase AKT has three isoforms (AKT1, AKT2, and AKT3) and transduces signals by phosphorylating downstream targets. AKT has profound protective effects on the cardiovascular system [15] through its ability to promote cardiac or vascular cell survival [16–19] and activate endothelial nitric oxide synthase [20]. However, AKT, especially the AKT2 isoform, has a potent role in promoting platelet activation and arterial thrombosis [21–26], although its role in venous thrombosis is less clear. In this study, we examined the role of AKT2 in venous thrombosis in mice and investigated AKT2's direct effects on the expression of coagulation factors in cultured endothelial cells. Our findings suggest that AKT2 may protect endothelial cells, regulate endothelial-mediated coagulation homeostasis, and promote intrathrombotic recanalization and subsequent thrombolysis. Thus, AKT2 plays comprehensive and dynamic roles in venous thrombus formation and resolution in a cell type-specific manner.

Methods

Mouse model of stenosis-induced DVT

All animal experiments were approved by the Institutional Animal Care and Use Committee at Baylor College of Medicine in accordance with the guidelines of the National Institutes of Health. Wild-type (WT) C57BL/6 J mice and B6.Cg-*Akt2*^{tm1.1Mbb}/J mice with a C57BL/6 J background (*Akt2*^{-/-}) [27] from The Jackson Laboratory (Bar Harbor, ME) were used.

Venous thrombus formation was induced in mice by using a mouse model of stenosis-induced DVT [7, 28].

Eight-week-old WT and *Akt2*^{-/-} male mice underwent general anesthesia (via inhalation of 2–3% isoflurane in an oxygen mix), and pain was managed by the subcutaneous injection of buprenorphine (a 1 mg/kg injection 30 min before surgery and then a 0.1–1.0 mg/kg injection every 12–24 h for 72–120 h). A midline laparotomy was performed, and the inferior vena cava (IVC) was identified. A 4–0 polypropylene suture was placed longitudinally along the ventral surface of the vein, and the IVC was ligated below the renal veins with a 7–0 polypropylene suture. The 4–0 polypropylene suture was then removed to avoid complete occlusion. Side branches were not ligated. Control mice underwent the same surgical procedures without IVC ligation (sham ligation). This procedure was performed under sterile conditions.

Mice were euthanized via inhalation of CO₂ at 1, 7, 14, 21, and 28 days after IVC ligation. The IVC with associated thrombus was harvested, and the combined weight of the thrombus and the vein wall from the thrombus-containing IVC was used to represent the weight of the thrombus. The IVC was then either fixed in formalin and embedded in paraffin for histologic analysis or embedded in optimal cutting temperature compound for immunofluorescence staining. For protein analysis, a portion of the IVC was snap frozen and stored at –80 °C. Six mice were analyzed at each time point for each group.

Immunofluorescence staining and quantification

Frozen sections were fixed with Cytfix (BD Biosciences, San Jose, CA), and cells were permeabilized with Perm/Wash (BD Biosciences). Nonspecific staining was reduced by blocking with 5% normal blocking serum. Sections were stained with primary antibody (Table 1) at room temperature for 2 h or at 4 °C overnight, followed by staining with secondary antibody conjugated to an Alexa Fluor dye (ie, Alexa Fluor 568 or 488; Invitrogen, Carlsbad, CA). Nuclei were counterstained with 4',6-diamidino-2-phenylindole dihydrochloride (DAPI). Slides incubated with secondary antibody only were used as negative controls. For immunohistochemistry and immunofluorescence studies, antibodies against tissue factor (TF), thrombomodulin (TM), endothelial protein C receptor (EPCR) (all from Santa Cruz Biotechnology, Santa Cruz, CA), AKT2, receptor-interacting protein kinase 3 (RIP3), vascular endothelial growth factor (VEGF) (all from Cell Signaling Technology, Danvers, MA), CD31, and Sm22- α (Abcam, Cambridge, MA) were used. Sections were examined by using an Olympus DP70 fluorescence microscope (Olympus, Tokyo, Japan). Images from 5 to 8 randomly selected visual fields (magnification, $\times 400$) per IVC section were captured, and the positive signal (positive cells or positive-staining area, without selecting autofluorescent elastic fibers) and the evaluated area were measured by using Image-Pro Plus V7.0 software (Media Cybernetics, Inc., Bethesda, MD). The positive signal was normalized to the evaluated IVC area, and the mean positive signals were calculated and compared between groups.

Apoptosis analysis with the terminal deoxynucleotidyl transferase–mediated dUTP–biotin nick end labeling (TUNEL) assay

Apoptosis was studied by using the TUNEL assay (Roche Applied Science, Indianapolis, IA). Briefly, frozen sections of IVC were fixed with 4% paraformaldehyde in phosphate-buffered saline (PBS) for 10 min and permeabilized with 0.2% Triton X-100 for 5 min. The fixed tissues were incubated for 1 h at 37 °C with TUNEL reaction mixture containing terminal deoxynucleotidyl transferase. Nuclei were counterstained with DAPI after TUNEL staining. Terminal deoxynucleotidyl transferase–free labeling mixture was used in negative control reactions. The capture of images and the quantification of positive cells were performed as described above.

Cell culture and transfection

Human umbilical vein endothelial cells (HUVECs) (Thermo Fisher Scientific Corporation, Waltham, MA) were cultured in endothelial cell culture media (Thermo Fisher Scientific Corporation) with 10% fetal bovine serum, endothelial cell growth factor (100 µg/mL), penicillin (100 U/mL), streptomycin (100 µg/mL), sodium pyruvate (1 mmol/L), L-glutamine (4 mmol/L), and heparin (30 µg/mL). HUVECs were transfected with plasmid DNA or siRNA by using Lipofectamine (Thermo Fisher Scientific Corporation) according to the manufacturer's instructions. Transfection efficiency was confirmed by means of Western blot analysis. AKT2 siRNA (#6396) and control siRNA (#6568) were from Cell Signaling Technology (Danvers, MA). WT-AKT2 plasmid (#9016) and control vector (#10792), WT-forkhead box protein O1 (FOXO1, #12142), constitutively active (CA)-FOXO1 (#12143), and dominant-negative (DN)-FOXO1 plasmids (#12145) were from Addgene Inc. (Cambridge, MA).

Western blot analysis

Treated cells were collected and lysed. Protein samples (15 µg per lane) were subjected to 10% sodium dodecyl sulfate polyacrylamide gel electrophoresis and were transferred to polyvinylidene fluoride membranes. The membranes were blocked, incubated with primary antibody (Table 1), washed, and incubated with secondary horse radish peroxidase–labeled antibody. Bands were visualized by using enhanced chemiluminescence (Bio-Rad, Hercules, CA). Protein bands, including those for β-actin, were quantified by using densitometry with the Quantity One imaging program (Bio-Rad). Protein levels were normalized to those of β-actin and expressed as the percentage of the no-treatment control.

Quantitative real–time polymerase chain reaction (qRT–PCR)

Total RNA from treated cells was extracted with Trizol (Invitrogen) according to the manufacturer's protocol. mRNA was reverse-transcribed with the iScript cDNA synthesis kit (Bio-Rad) according to the manufacturer's protocol. qRT-PCR was performed with SsoAdvanced Universal SYBR Green Supermix buffer (Bio-Rad). Primers were designed with Beacon Designer 2.0 software (Premier Biosoft International, Palo Alto, CA). Levels of mRNA were determined by normalizing the cycle threshold (Ct) of the target genes to the Ct of β-actin. The relative levels of mRNA were compared and expressed as the percentage of the no-treatment control. The primers for human *TM* mRNA were as follows [29]: forward:

5'-CAGTGGGTTACGGGAGACAA-3'; and reverse: 5'-CCTTCACTTCGCACTGCTGC-3'. The primers for human *TF* mRNA were as follows [30]: forward: 5'-AATGTGGAGAGCACCGGTTTC-3'; and reverse: 5'-CCGTTTCATCTTCTACGGTCA-3'. The primers for glyceraldehyde-3-phosphate dehydrogenase (GAPDH) were as follows: forward, 5'-CATGTTTCGTCATGGGTGTGAACCA-3'; and reverse, 5'-AGTGATGGCATGGACTGTGGTCAT-3'.

Statistical analysis

All quantitative data are presented as the mean \pm standard deviation (SD). Data were analyzed with GraphPad (Graph-Pad Prism 8.1.2). Normality of the data was examined by using the Kolmogorov–Smirnov test. The independent *t* test, one-way analysis of variance (ANOVA), and two-way ANOVA were used to compare normally distributed values, whereas the Mann–Whitney test or the Kruskal–Wallis test was performed to compare data without a normal distribution. For multiple group comparisons, P-values were obtained by performing post-hoc pairwise comparisons with the Bonferroni correction, the Tukey multiple comparisons test, and the Holm–Sidak multiple comparisons test. For all statistical analyses, 2-tailed probability values were used.

Results

Reduced thrombus resolution in the ligated IVC of *Akt2*^{-/-} mice

To study the role of AKT2 in venous thrombosis, we used a mouse model of venous thrombosis induced by IVC ligation and subsequent flow restriction and stenosis (Fig. 1a). We first examined the effect of IVC ligation on AKT2 expression. In WT mice, AKT2 was detected in sham-ligated IVCs, but its level was significantly higher in ligated IVCs (Fig. 1b), suggesting that AKT2 expression was induced by IVC ligation. To determine whether the upregulation of AKT2 plays a protective or detrimental role in the development of venous thrombosis, we compared thrombus formation and resolution between WT mice and *Akt2*^{-/-} mice. In WT mice, venous thrombi formed after ligation, remained at the same size and weight at day 7, gradually decreased in size and weight at days 14 and 21, and completely resolved by day 28 (Fig. 1c, d). However, in *Akt2*^{-/-} mice, the thrombi in the ligated IVC were significantly larger than those in the ligated IVC of WT mice at day 7 and remained unresolved at days 14, 21, and 28. This suggested that *Akt2*^{-/-} mice had minimal effects on thrombus formation at the early stage (ie, day 1) but had impaired thrombus resolution at the later stages (ie, days 7, 14, 21, and 28) examined. These data indicate that AKT2 may play a role in promoting thrombus resolution.

Increased TF and reduced TM expression in the ligated IVC of *Akt2*^{-/-} mice

To determine the potential mechanism(s) for increased venous thrombosis in *Akt2*^{-/-} mice, we compared the expression of prothrombotic TF and antithrombotic TM and EPCR in the ligated IVC between WT mice and *Akt2*^{-/-} mice 2 weeks after ligation. In WT mice, IVC ligation increased TF expression (Fig. 2a). However, ligation-induced TF expression was even more prominent in *Akt2*^{-/-} mice than that in WT mice. TF was highly expressed inside thrombus and in the thrombotic wall of *Akt2*^{-/-} mice. Compared with sham ligation, IVC

ligation also increased the expression of TM (Fig. 2b) in WT mice. However, this IVC ligation-induced increase in TM expression was severely compromised in *Akt2*^{-/-} mice (Fig. 2b). Similarly, compromised EPCR expression (Fig. 2c) was also observed in *Akt2*^{-/-} mice. This prothrombotic feature seen in the IVC of *Akt2*^{-/-} mice suggests that AKT2 may play a role in regulating venous coagulation homeostasis.

Increased cell death in the ligated IVC of *Akt2*^{-/-} mice

We also analyzed apoptosis and necroptosis [31], two important mechanisms in tissue damage, in the ligated IVC of *Akt2*^{-/-} and WT mice 2 weeks after ligation. As shown in Fig. 3a, TUNEL-positive cells were observed in the ligated IVC of WT mice. However, the number of TUNEL-positive cells was significantly higher in the ligated IVC of *Akt2*^{-/-} mice than in that of WT mice. Apoptotic cells were particularly abundant inside the thrombus of the ligated IVC in *Akt2*^{-/-} mice. Additionally, RIP3, the key molecule in the necroptosis pathway [31], was detected in the thrombi and vascular wall of the ligated IVC in *Akt2*^{-/-} mice (Fig. 3b). The increased apoptosis and activation of the necroptosis pathway observed in the ligated IVC of *Akt2*^{-/-} mice suggests that AKT2 may protect the vein wall by preventing necroptotic and apoptotic cell death.

Reduced intrathrombotic angiogenesis and recanalization in the ligated IVC of *Akt2*^{-/-} mice

Intrathrombotic recanalization is essential for thrombus resolution [13, 14]. Interestingly, although there was an abundance of intrathrombotic CD31 cells in the ligated IVC of *Akt2*^{-/-} mice, these cells failed to form organized small vessels. The number of intrathrombotic CD31-positive channels was significantly lower in the IVC of *Akt2*^{-/-} mice than in that of WT mice (Fig. 4a). Furthermore, the intrathrombotic expression of angiogenic VEGF was significantly lower in the IVC of *Akt2*^{-/-} mice than in that of WT mice (Fig. 4b). The impaired intrathrombotic angiogenesis and delayed venous thrombus resolution in *Akt2*^{-/-} mice imply that AKT2 may increase intrathrombotic recanalization and promote thrombus resolution.

Increased fibrotic remodeling in the ligated IVC of *Akt2*^{-/-} mice

Unresolved thrombus can trigger fibrotic changes. Indeed, when we examined the presence of fibroblast specific protein-1 (Fsp-1)-positive fibroblasts in the IVC 2 weeks after ligation, we detected significantly more fibroblasts in *Akt2*^{-/-} mice than in WT mice (Fig. 4c). The fibroblasts were observed both inside thrombus and in the vein wall. Double staining with the smooth muscle cell marker Sm22- α showed that many smooth muscle cells in the vein wall and thrombus also expressed Fsp-1 (Fig. 4d), suggesting the potential transformation from smooth muscle cells to fibroblasts. Furthermore, the expression of the fibrotic transforming growth factor (TGF)- β and downstream transcription factor Smad3 were markedly increased in the ligated IVC of *Akt2*^{-/-} mice compared with that of WT mice (Fig. 4e).

AKT2 upregulates TM expression and downregulates TF expression via the inhibition of FOXO1

Because we observed increased TF and reduced TM expression in the ligated IVC of *Akt2*^{-/-} mice, we investigated the mechanism underlying the AKT2-mediated regulation of venous homeostasis. We observed that overexpression of WT-AKT2 increased TM protein and *TM* mRNA levels, whereas AKT2 siRNA decreased TM protein and *TM* mRNA (Fig. 5a, b) levels. In contrast, WT-AKT2 decreased TF protein and *TF* mRNA levels, whereas AKT2 siRNA increased TF protein and *TF* mRNA levels (Fig. 5a, b), suggesting that AKT2 enhances TM expression and inhibits TF expression.

To further understand the mechanism underlying the AKT2-mediated regulation of TM and TF expression, we examined whether the expression of TM and TF can be regulated by the transcription factor FOXO1, a major AKT target that can be directly phosphorylated and inhibited by AKT. Indeed, as shown in Fig. 5c, overexpression of WT FOXO1 (WT-FOXO1) and constitutively active FOXO1 (CA-FOXO1) decreased *TM* mRNA levels, whereas dominant negative FOXO1 (DN-FOXO1) increased *TM* mRNA levels. In contrast, WT-FOXO1 and CA-FOXO1, but not DN-FOXO1, increased *TF* mRNA levels. A similar pattern of TM and TF regulation by FOXO1 was also observed at the protein level (data not shown).

Importantly, WT-AKT2 reduced the inhibition of *TM* mRNA expression and the stimulation of *TF* mRNA expression induced by FOXO1 (Fig. 5d). Together, these findings suggest that AKT2 regulates TM and TF expression by interfering with the FOXO1-mediated regulation of TM and TF.

Discussion

In this study, we report a potentially protective role of AKT2 against venous thrombosis. We found that *Akt2* deficiency in mice not only increased susceptibility to ligation-induced coagulation disturbance and endothelial injury, but it also delayed intrathrombus recanalization and thrombus resolution, leading to venous fibrotic remodeling. Furthermore, we found that by inhibiting the transcription factor FOXO1, AKT2 promoted TM expression and suppressed TF expression in human endothelial cells. Our results suggest that AKT2 may play dynamic roles in venous thrombus formation and resolution.

Venous thromboembolism is multifactorial and is often triggered by an array of genetic and clinical risk factors [3, 32–34]. These factors promote venous thrombosis by altering blood flow, inducing endothelial dysfunction, activating inflammatory cells, and dysregulating coagulation factors that lead to increased blood coagulation and impaired thrombolysis. However, how these genetic and clinical risk factors trigger pathologic processes is not completely understood at the molecular level. In this study, we show that AKT2 protects the vein wall against DVT formation. Although *Akt2*^{-/-} mice did not develop spontaneous venous thrombosis in the absence of exogenous stress, they showed markedly increased susceptibility to ligation-induced venous thrombosis with features of increased coagulation and endothelial injury, delayed intrathrombus recanalization and resolution, and profound fibrotic remodeling.

Several mechanisms may account for the protective effects of AKT2 against venous thrombosis. Here, we show that AKT2 may protect against venous thrombosis by regulating the balance between coagulation and anticoagulation. We observed significantly increased TF expression and compromised TM induction in the ligated IVC of *Akt2*^{-/-} mice. In cultured endothelial cells, AKT2 promoted TM expression and inhibited TF expression, which is consistent with previous reports [35, 36]. Moreover, we found that the transcription factor FOXO1, downstream of AKT, downregulated TM expression and upregulated TF expression. By inhibiting FOXO1, AKT stimulated TM expression and inhibited TF expression. Other mechanisms may also contribute to the protective effects of AKT2 against venous thrombosis. We observed a significant increase in the number of apoptotic cells and the activation of necroptosis in the lesion regions in the IVC of *Akt2*^{-/-} mice, indicating that AKT may protect vascular cells of the vein wall. AKT has well-established roles in promoting cell survival [17, 37] by directly inhibiting apoptosis signal-regulating kinase 1 [38], p53 [38], and Bcl-2-associated death promoter (BAD) [39]. Thus, protecting vascular cells, especially endothelial cells, may contribute to AKT2's protective effects against venous thrombosis.

We also observed significantly impaired thrombus resolution in *Akt2*^{-/-} mice. The regulation of venous thrombus resolution is poorly understood. Several lines of evidence suggest that intrathrombus angiogenesis promotes thrombus resolution [12]. Factors that induce thrombus resolution do so by increasing angiogenesis and VEGF expression [10]. Mice with the endothelial cell-specific deletion of the VEGF receptor and thus defective angiogenesis show delayed thrombus resolution [13]. Furthermore, anti-angiogenic therapy inhibits venous thrombus resolution [14]. The significant defect in angiogenesis and recanalization observed in *Akt2*^{-/-} mice indicates that AKT2 may promote thrombus resolution by promoting intrathrombus angiogenesis. However, it remains to be determined how angiogenesis promotes thrombus resolution. It has been proposed that the recruitment of inflammatory cells may play a role [10]. Other mechanisms such as the improvement of oxygen supply may also play a role. Future studies are required to understand the mechanisms involved in thrombus resolution. Finally, we also observed a significant increase in the number of fibroblasts and in the activation of TGF- β signaling in the ligated IVC of *Akt2*^{-/-} mice. This fibrosis remodeling may be caused by unresolved injury and chronic inflammation. However, AKT2 may also directly inhibit TGF- β signaling [40, 41], a critical player in fibrotic remodeling.

It is noteworthy that AKT2's cell-specific actions (e.g., in platelets vs endothelial cells) may explain its differential roles in arterial and venous thrombosis. Although a recent study showed that the AKT signaling pathway mediates the adenosine-induced inhibition of thrombus formation [36], most studies show that all 3 AKT isoforms are critically involved in arterial thrombosis [21–23]. However, our study suggests that AKT2 has a protective role against venous thrombosis. The cell-specific functions of AKT2 in thrombus formation and resolution may explain its dynamic roles in arterial and venous thrombosis. In platelets, AKT has prothrombotic functions [24–26], including the promotion of platelet aggregation, fibrinogen binding, and granule secretion [22]. In contrast, in endothelial cells, we show that AKT2 has a protective role in sustaining cell survival, regulating coagulation homeostasis, and promoting intrathrombotic recanalization, which may reduce thrombus formation and

enhance thrombus resolution. Whereas AKT-mediated platelet activation may play a critical role in arterial thrombosis, the AKT-mediated protection of endothelial function may prevent venous thrombus formation and promote thrombus resolution.

Because of the diverse roles of AKT2 in endothelial cells, platelets, and inflammatory cells, the overall effect of AKT2 on venous thrombosis formation and resolution is most likely to be dynamic and stage dependent. AKT2 may promote platelet-mediated thrombus formation at an early stage but promote angiogenesis-dependent thrombus resolution at a later stage. Therefore, the difference in thrombus size between *Akt2*^{-/-} mice and WT mice is probably dynamic. Understanding AKT2's precise control of thrombosis and thrombolysis kinetics requires further studies. In addition, studies in mice with the cell-specific (i.e., platelets vs endothelial cells) deletion of *AKT* are needed to further dissect the cell-specific roles of all 3 isoforms of AKT in venous coagulation and in thrombus formation and resolution, in both male and female mice.

AKT signaling is often compromised in patients with insulin resistance/diabetes [42] or inflammation [43], as well as in patients undergoing chemotherapy; notably, these patients are prone to venous thrombosis [32, 44–46]. The pro-venous thrombosis feature of *Akt2* deficiency may explain the mechanism underlying increased venous thrombosis in patients with these conditions. Diabetes is associated with increased levels of free fatty acids, which have been shown to inhibit AKT signaling, leading to endothelial dysfunction [42, 43]. Insulin/AKT signaling resistance in the vascular wall may be partially responsible for the increased venous thrombosis observed in patients with diabetes [34, 47, 48]. Chronic inflammation and associated inflammatory factors also inhibit AKT signaling [42, 43]. In addition, chronic inflammation exists in disease conditions such as cancer, which is a major risk factor for venous thrombosis [49]. Cancer treatment and anti-angiogenic therapy that target AKT have been shown to promote venous thrombosis and impair thrombus resolution [14]. Thus, the impaired AKT signaling observed in the presence of obesity, inflammation, or anticancer therapy may contribute to venous thrombosis in patients with these conditions.

In conclusion, our findings suggest that AKT2 protects endothelial cells from death, regulates endothelial-mediated coagulation homeostasis, and promotes intrathrombotic recanalization and thrombolysis. Thus, AKT2 potentially plays dynamic and tissue-specific roles in venous thrombus formation and resolution. Reduced AKT signaling in endothelial cells may contribute to venous thrombosis in conditions such as diabetes, inflammation, and anticancer therapy. Future studies are warranted to dissect the cell-specific roles of AKT2.

Acknowledgments

We gratefully acknowledge Nicole Stancel, PhD, ELS(D), for editorial support. This work was supported by the American Heart Association (AHA-0730190 N, HL-HL131980 and HL143359 to Y.H.S.) and The National Key Technology R&D Program of the Ministry of Science and Technology (2012BAI05B02 to C.W.).

References

1. Hansson PO, Welin L, Tibblin G, Eriksson H (1997) Deep vein thrombosis and pulmonary embolism in the general population. 'The study of men born in 1913'. Arch Intern Med 157:1665–1670 [PubMed: 9250227]

2. Heit JA, Silverstein MD, Mohr DN, Petterson TM, O'Fallon WM, Melton LJ 3rd (1999) Predictors of survival after deep vein thrombosis and pulmonary embolism: a population-based, cohort study. *Arch Intern Med* 159:445–453 [PubMed: 10074952]
3. White RH (2003) The epidemiology of venous thromboembolism. *Circulation* 107:14–8 [PubMed: 12814979]
4. Kearon C (2003) Natural history of venous thromboembolism. *Circulation* 107:122–30
5. Kahn SR, Shrier I, Julian JA et al. (2008) Determinants and time course of the postthrombotic syndrome after acute deep venous thrombosis. *Ann Intern Med* 149:698–707 [PubMed: 19017588]
6. Pepke-Zaba J, Delcroix M, Lang I et al. (2011) Chronic thromboembolic pulmonary hypertension (CTEPH): results from an international prospective registry. *Circulation* 124:1973–1981 [PubMed: 21969018]
7. Henke PK, Varga A, De S et al. (2004) Deep vein thrombosis resolution is modulated by monocyte CXCR2-mediated activity in a mouse model. *Arterioscler Thromb Vasc Biol* 24:1130–1137 [PubMed: 15105284]
8. Henke PK, Pearce CG, Moaveni DM et al. (2006) Targeted deletion of CCR2 impairs deep vein thrombosis resolution in a mouse model. *J Immunol* 177:3388–3397 [PubMed: 16920980]
9. Henke PK, Mitsuya M, Luke CE et al. (2011) Toll-like receptor 9 signaling is critical for early experimental deep vein thrombosis resolution. *Arterioscler Thromb Vasc Biol* 31:43–49 [PubMed: 20966396]
10. Nosaka M, Ishida Y, Kimura A et al. (2011) Absence of IFN-gamma accelerates thrombus resolution through enhanced MMP-9 and VEGF expression in mice. *J Clin Invest* 121:2911–2920 [PubMed: 21646723]
11. Henke PK, Varma MR, Moaveni DK et al. (2007) Fibrotic injury after experimental deep vein thrombosis is determined by the mechanism of thrombogenesis. *Thromb Haemost* 98:1045–1055 [PubMed: 18000610]
12. Wakefield TW, Myers DD, Henke PK (2008) Mechanisms of venous thrombosis and resolution. *Arterioscler Thromb Vasc Biol* 28:387–391 [PubMed: 18296594]
13. Alias S, Redwan B, Panzenbock A et al. (2014) Defective angiogenesis delays thrombus resolution: a potential pathogenetic mechanism underlying chronic thromboembolic pulmonary hypertension. *Arterioscler Thromb Vasc Biol* 34:810–819 [PubMed: 24526692]
14. Evans CE, Grover SP, Humphries J et al. (2014) Antiangiogenic therapy inhibits venous thrombus resolution. *Arterioscler Thromb Vasc Biol* 34:565–570 [PubMed: 24436367]
15. Shiojima I, Walsh K (2002) Role of Akt signaling in vascular homeostasis and angiogenesis. *Circ Res* 90:1243–1250 [PubMed: 12089061]
16. Condorelli G, Drusco A, Stassi G et al. (2002) Akt induces enhanced myocardial contractility and cell size in vivo in transgenic mice. *Proc Natl Acad Sci USA* 99:12333–12338 [PubMed: 12237475]
17. Fujio Y, Nguyen T, Wencker D, Kitsis RN, Walsh K (2000) Akt promotes survival of cardiomyocytes in vitro and protects against ischemia-reperfusion injury in mouse heart. *Circulation* 101:660–667 [PubMed: 10673259]
18. Matsui T, Tao J, del Monte F et al. (2001) Akt activation preserves cardiac function and prevents injury after transient cardiac ischemia in vivo. *Circulation* 104:330–335 [PubMed: 11457753]
19. Shen YH, Zhang L, Ren P et al. (2013) AKT2 confers protection against aortic aneurysms and dissections. *Circ Res* 112:618–632 [PubMed: 23250987]
20. Luo Z, Fujio Y, Kureishi Y et al. (2000) Acute modulation of endothelial Akt/PKB activity alters nitric oxide-dependent vasomotor activity in vivo. *J Clin Invest* 106:493–499 [PubMed: 10953024]
21. Chen J, De S, Damron DS, Chen WS, Hay N, Byzova TV (2004) Impaired platelet responses to thrombin and collagen in AKT-1-deficient mice. *Blood* 104:1703–1710 [PubMed: 15105289]
22. Woulfe D, Jiang H, Morgans A, Monks R, Birnbaum M, Brass LF (2004) Defects in secretion, aggregation, and thrombus formation in platelets from mice lacking Akt2. *J Clin Invest* 113:441–450 [PubMed: 14755341]
23. O'Brien KA, Stojanovic-Terpo A, Hay N, Du X (2011) An important role for Akt3 in platelet activation and thrombosis. *Blood* 118:4215–4223 [PubMed: 21821713]

24. Martin V, Guillermet-Guibert J, Chicanne G et al. (2011) Deletion of the p110beta isoform of phosphoinositide 3-kinase in platelets reveals its central role in Akt activation and thrombus formation in vitro and in vivo. *Blood* 115:2008–2013
25. Patel S, Huang YW, Reheman A et al. (2012) The cell motility modulator Slit2 is a potent inhibitor of platelet function. *Circulation* 126:1385–1395 [PubMed: 22865890]
26. Borst O, Munzer P, Gatidis S et al. (2012) The inflammatory chemokine CXC motif ligand 16 triggers platelet activation and adhesion via CXC motif receptor 6-dependent phosphatidylinositide 3-kinase/Akt signaling. *Circ Res* 111:1297–1307 [PubMed: 22927331]
27. Cho H, Mu J, Kim JK et al. (2001) Insulin resistance and a diabetes mellitus-like syndrome in mice lacking the protein kinase Akt2 (PKB beta). *Science* 292:1728–1731 [PubMed: 11387480]
28. Diaz JA, Obi AT, Myers DD Jr et al. (2012) Critical review of mouse models of venous thrombosis. *Arterioscler Thromb Vasc Biol* 32:556–562 [PubMed: 22345593]
29. Rong Y, Zhang M, Zhang L, Wang XL, Shen YH (2010) JNKATF-2 inhibits thrombomodulin (TM) expression by recruiting histone deacetylase4 (HDAC4) and forming a transcriptional repression complex in the TM promoter. *FEBS Lett* 584:852–858 [PubMed: 20116378]
30. Wang JG, Geddings JE, Aleman MM et al. (2012) Tumor-derived tissue factor activates coagulation and enhances thrombosis in a mouse xenograft model of human pancreatic cancer. *Blood* 119:5543–5552 [PubMed: 22547577]
31. Vandenabeele P, Galluzzi L, Vanden Berghe T, Kroemer G (2010) Molecular mechanisms of necroptosis: an ordered cellular explosion. *Nat Rev Mol Cell Biol* 11:700–714 [PubMed: 20823910]
32. Heit JA, Silverstein MD, Mohr DN, Petterson TM, O’Fallon WM, Melton LJ 3rd (2000) Risk factors for deep vein thrombosis and pulmonary embolism: a population-based case-control study. *Arch Intern Med* 160:809–815 [PubMed: 10737280]
33. Heit JA (2008) The epidemiology of venous thromboembolism in the community. *Arterioscler Thromb Vasc Biol* 28:370–372 [PubMed: 18296591]
34. Parkin L, Sweetland S, Balkwill A, Green J, Reeves G, Beral V (2012) Body mass index, surgery, and risk of venous thromboembolism in middle-aged women: a cohort study. *Circulation* 125:1897–1904 [PubMed: 22394567]
35. Ramachandran A, Ranpura SA, Gong EM, Mulone M, Cannon GM Jr, Adam RM (2010) An Akt- and Fra-1-dependent pathway mediates platelet-derived growth factor-induced expression of thrombomodulin, a novel regulator of smooth muscle cell migration. *Am J Pathol* 177:119–131 [PubMed: 20472895]
36. Zhang W, Wang J, Wang H et al. (2010) Acadesine inhibits tissue factor induction and thrombus formation by activating the phosphoinositide 3-kinase/Akt signaling pathway. *Arterioscler Thromb Vasc Biol* 30:1000–1006 [PubMed: 20185792]
37. Amaravadi R, Thompson CB (2005) The survival kinases Akt and Pim as potential pharmacological targets. *J Clin Invest* 115:2618–2624 [PubMed: 16200194]
38. Kim AH, Khursigara G, Sun X, Franke TF, Chao MV (2001) Akt phosphorylates and negatively regulates apoptosis signal-regulating kinase 1. *Mol Cell Biol* 21:893–901 [PubMed: 11154276]
39. Datta SR, Dudek H, Tao X et al. (1997) Akt phosphorylation of BAD couples survival signals to the cell-intrinsic death machinery. *Cell* 91:231–241 [PubMed: 9346240]
40. Conery AR, Cao Y, Thompson EA, Townsend CM Jr, Ko TC, Luo K (2004) Akt interacts directly with Smad3 to regulate the sensitivity to TGF-beta induced apoptosis. *Nat Cell Biol* 6:366–372 [PubMed: 15104092]
41. Remy I, Montmarquette A, Michnick SW (2004) PKB/Akt modulates TGF-beta signalling through a direct interaction with Smad3. *Nat Cell Biol* 6:358–365 [PubMed: 15048128]
42. Wang XL, Zhang L, Youker K et al. (2006) Free fatty acids inhibit insulin signaling-stimulated endothelial nitric oxide synthase activation through upregulating PTEN or inhibiting Akt kinase. *Diabetes* 55:2301–2310 [PubMed: 16873694]
43. Shen YH, Zhang L, Gan Y et al. (2006) Up-regulation of PTEN (phosphatase and tensin homolog deleted on chromosome ten) Mediates p38 MAPK Stress Signal-induced Inhibition of Insulin Signaling. A cross-talk between stress signaling and insulin signaling in resistent-treated human endothelial cells. *J Biol Chem* 281:7727–7736 [PubMed: 16418168]

44. Heit JA, O'Fallon WM, Petterson TM et al. (2002) Relative impact of risk factors for deep vein thrombosis and pulmonary embolism: a population-based study. *Arch Intern Med* 162:1245–1248 [PubMed: 12038942]
45. Braekkan SK, Hald EM, Mathiesen EB et al. (2012) Competing risk of atherosclerotic risk factors for arterial and venous thrombosis in a general population: the Tromso study. *Arterioscler Thromb Vasc Biol* 32:487–491 [PubMed: 22075253]
46. Roach RE, Lijfering WM, Flinterman LE, Rosendaal FR, Cannegieter SC (2013) Increased risk of CVD after VT is determined by common etiologic factors. *Blood* 121:4948–4954 [PubMed: 23645837]
47. Sanchez C, Poggi M, Morange PE et al. (2012) Diet modulates endogenous thrombin generation, a biological estimate of thrombosis risk, independently of the metabolic status. *Arterioscler Thromb Vasc Biol* 32:2394–2404 [PubMed: 22859493]
48. Owens AP 3rd, Byrnes JR, Mackman N (2014) Hyperlipidemia, tissue factor, coagulation, and simvastatin. *Trends Cardiovasc Med* 24:95–98 [PubMed: 24016468]
49. Timp JF, Braekkan SK, Versteeg HH, Cannegieter SC (2013) Epidemiology of cancer-associated venous thrombosis. *Blood* 122:1712–1723 [PubMed: 23908465]

Highlights

- Understanding the mechanisms of venous thrombus formation and resolution is critical for improving the management of venous thromboembolism, which carries a high risk of morbidity and mortality.
- In a mouse model of venous thrombosis induced by inferior vena cava (IVC) ligation, *Akt2* deficiency delayed thrombus resolution.
- The ligated IVC in *Akt2*^{-/-} mice displayed increased apoptosis and necroptosis, impaired recanalization and thrombus resolution, and increased fibrotic remodeling.
- These observations suggest a protective role of AKT2 in venous thrombus formation and resolution.

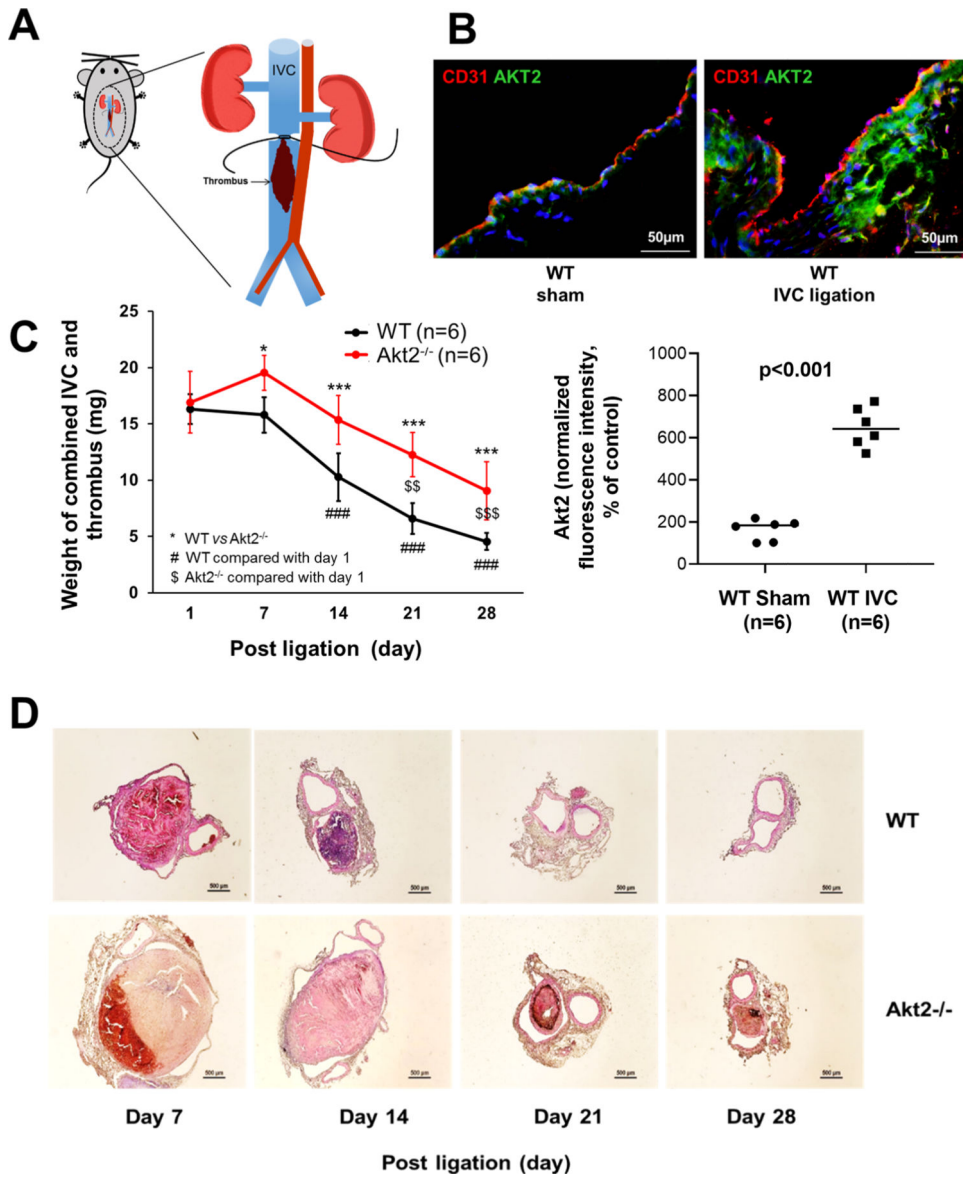
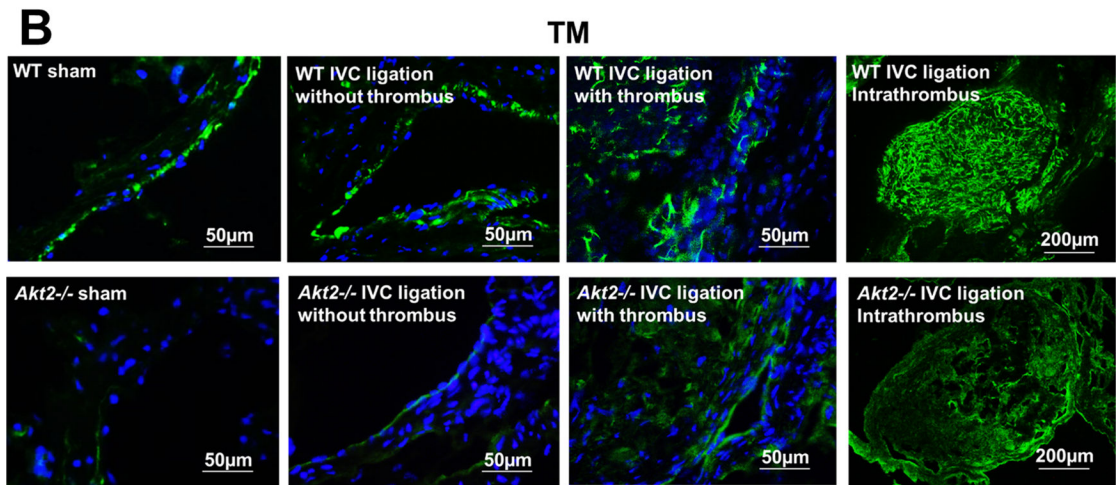
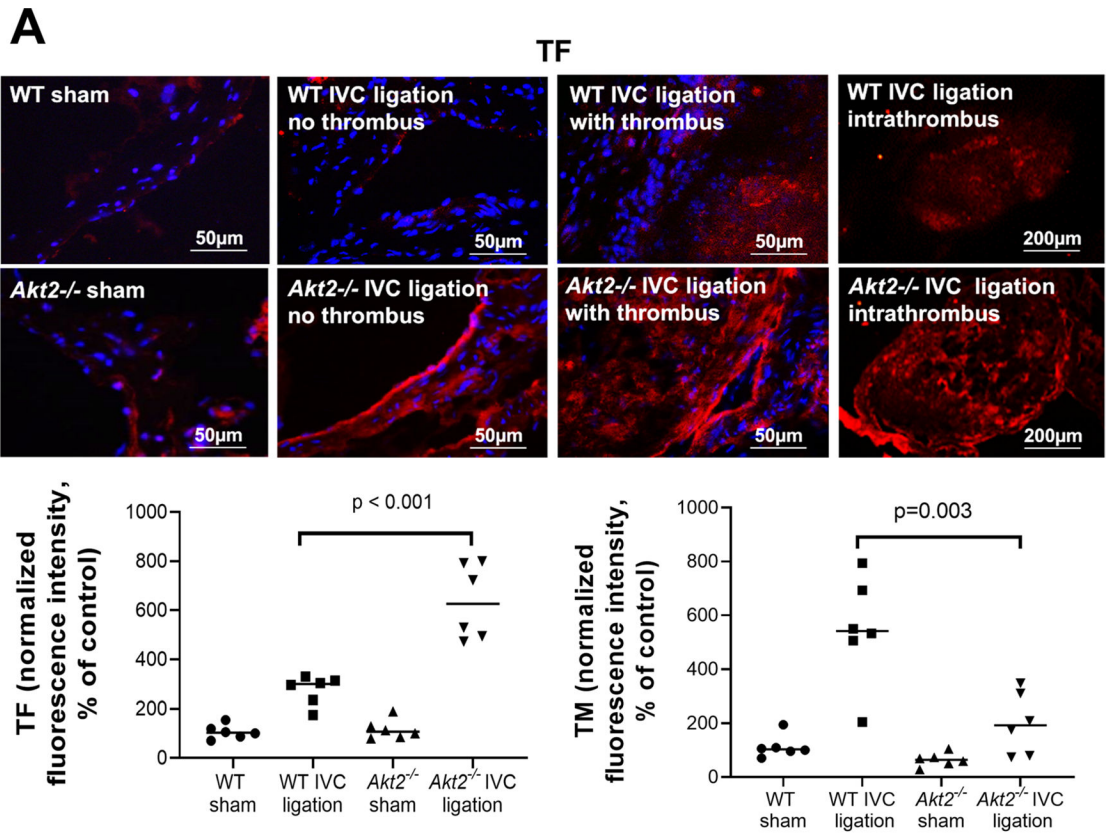


Fig. 1. Increased thrombus formation and impaired thrombus resolution in the ligated inferior vena cava (IVC) of *Akt2*^{-/-} mice. Wild-type (WT) mice and *Akt2*^{-/-} mice underwent a sham operation or IVC ligation. The thrombus-containing IVC was harvested from each mouse at the designated time. **a** Schematic illustration of IVC ligation. A midline laparotomy was performed, and the IVC was identified. A 4–0 polypropylene suture was placed longitudinally along the ventral surface of the vein, and the IVC was ligated below the renal veins with a 7–0 polypropylene suture. The 4–0 polypropylene suture was then removed to avoid complete occlusion. Side branches were not ligated. Control mice underwent the same surgical procedure without IVC ligation (sham ligation). **b** Representative images of immunofluorescence staining and quantification showing that IVC ligation increased AKT2 expression in the IVC of WT mice 1 week after ligation. For the quantification of staining, the mean positive-staining area was normalized with the evaluated area. All values represent

the mean (n = 6 per group). P-values were obtained by performing the Welch's *t* test. **c** Time-course analysis showing that the mean weight of the combined IVC and thrombus was significantly greater in *Akt2*^{-/-} mice than in WT mice from day 7 to day 28 after ligation. Furthermore, the mean weight of the combined IVC and thrombus decreased more slowly in *Akt2*^{-/-} mice (significantly reduced at day 21 after ligation) than in WT mice (significantly reduced at day 14 after ligation). All values represent the mean (n = 6 per group). P-values were obtained by performing two-way ANOVA analysis followed by post-hoc pairwise comparisons with the Bonferroni correction. **d** Representative hematoxylin and eosin staining showing larger thrombi in the IVC of *Akt2*^{-/-} mice than in that of WT mice at different times after ligation



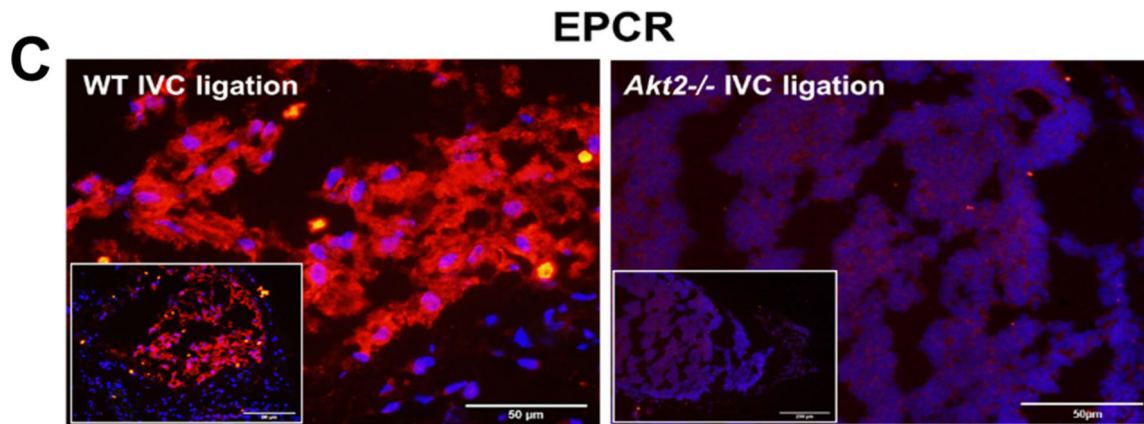


Fig. 2. Significantly increased tissue factor (TF) expression and decreased thrombomodulin (TM) expression in the ligated inferior vena cava (IVC) of *Akt2*^{-/-} mice. Wild-type (WT) mice and *Akt2*^{-/-} mice underwent a sham operation or IVC ligation. The thrombus-containing IVC was harvested from each mouse 2 weeks after ligation. Representative images of immunofluorescence staining and quantification showing increased TF expression (**a**) and decreased TM expression (**b**) in the ligated IVC of *Akt2*^{-/-} mice. For the quantification of staining, the mean positive-staining area was normalized with the evaluated area. All values represent the mean (n = 6 per group). P-values were obtained by performing multiple comparisons in one-way ANOVA analysis followed by the Tukey multiple comparisons test. **c** Representative images of immunofluorescence staining showing decreased endothelial protein C receptor (EPCR) expression in the ligated IVC of *Akt2*^{-/-} mice

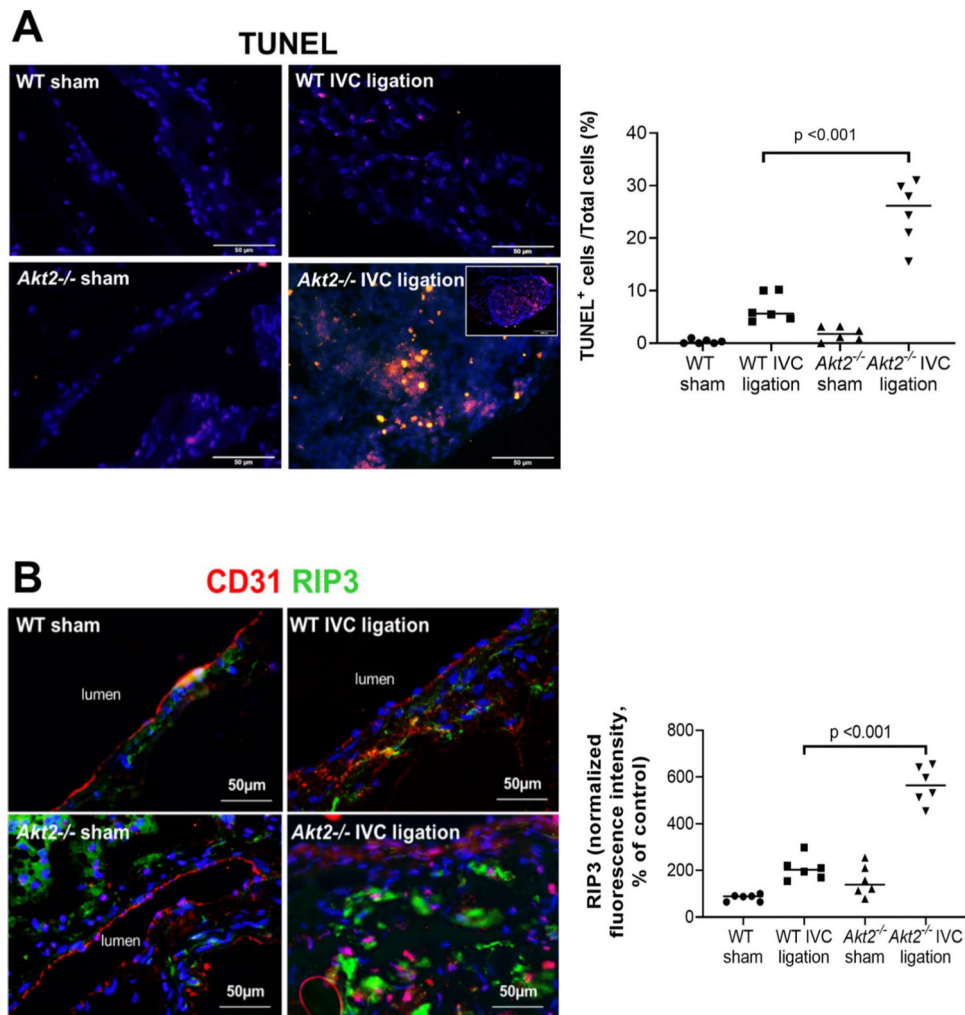
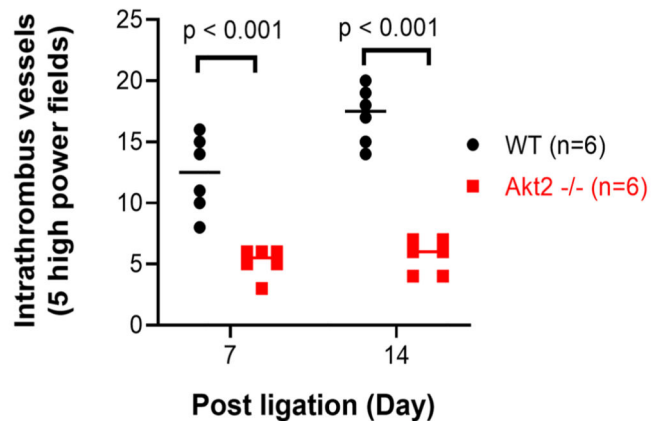
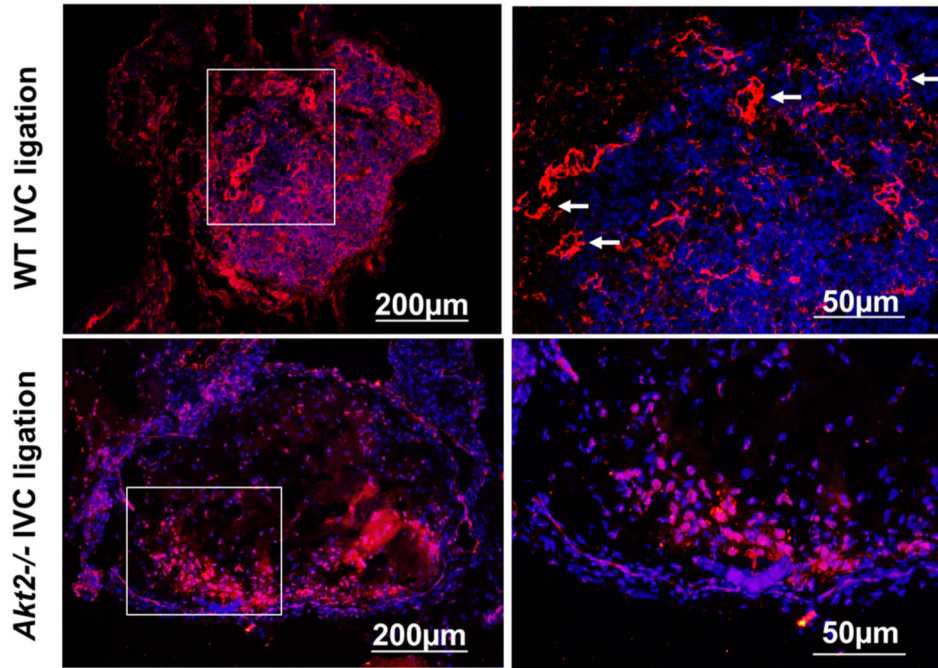
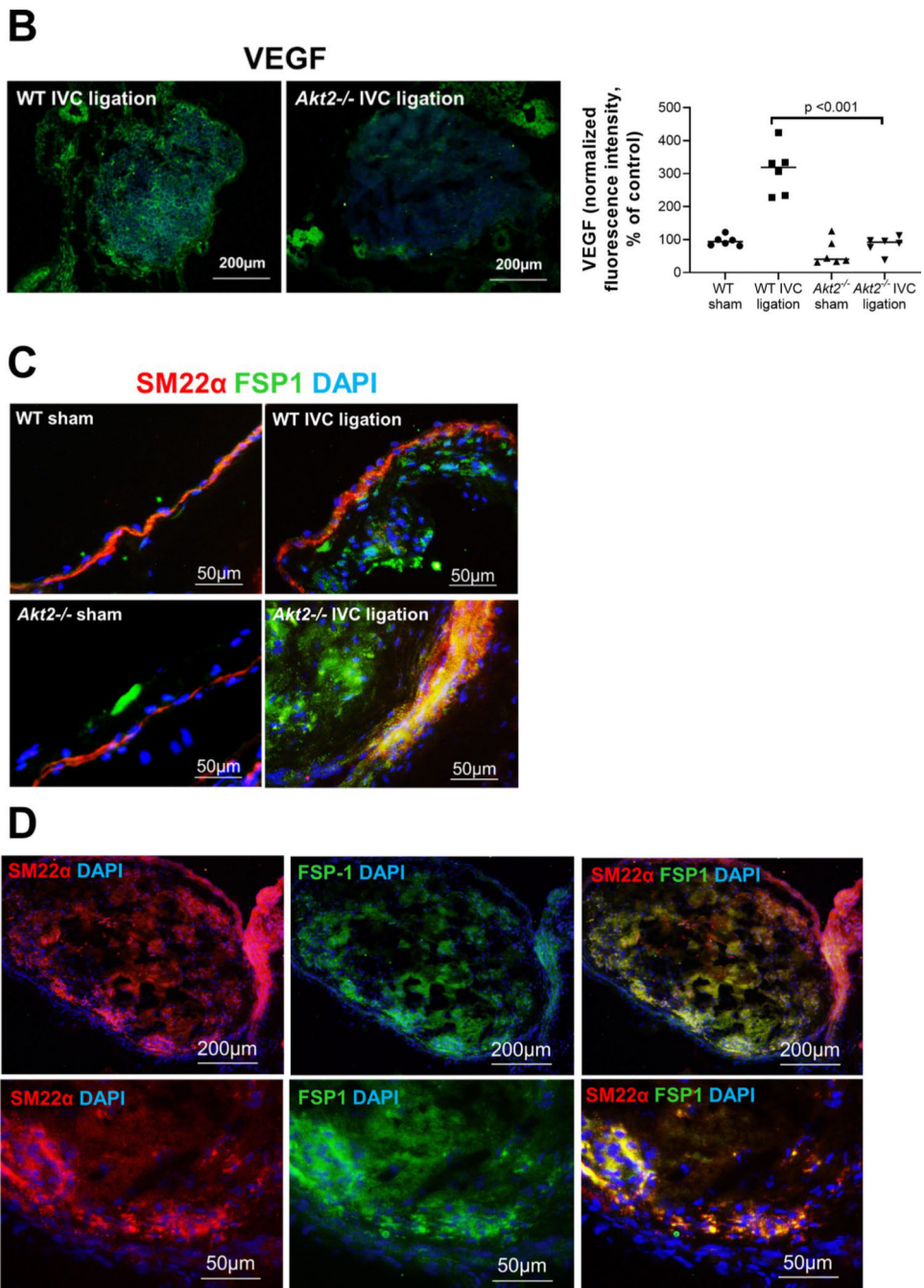
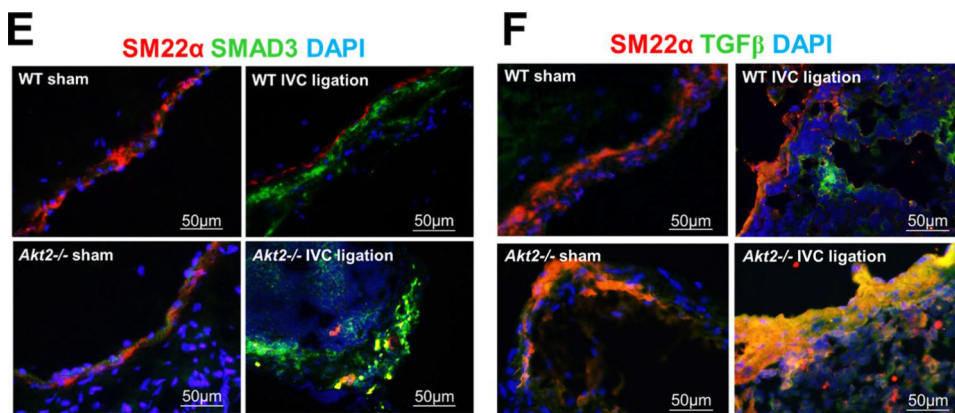


Fig. 3. Significantly increased cell death in the ligated inferior vena cava (IVC) of *Akt2*^{-/-} mice. Wild-type (WT) mice and *Akt2*^{-/-} mice underwent a sham operation or IVC ligation. The thrombus-containing IVC was harvested at 2 weeks after ligation. **a** Representative images of terminal deoxynucleotidyl transferase dUTP nick end labeling (TUNEL) staining and quantification showing that apoptosis was significantly increased in the lesion areas of the ligated IVC of *Akt2*^{-/-} mice, particularly in thrombus areas. For the quantification of staining, the number of TUNEL-positive cells was normalized to the total number of cells evaluated. All values represent the mean (n = 6 in each group). P-values were obtained by performing one-way ANOVA analysis followed by the Holm-Sidak multiple comparisons test. **b** Representative images of immunofluorescence staining and quantification showing a significant increase in the levels of the necroptosis molecule receptor-interacting protein kinase 3 (RIP3) in the ligated IVC of *Akt2*^{-/-} mice. For the quantification of staining, the mean positive-staining area was normalized with the evaluated aortic area. All values represent the mean (n = 6 per group). P-values were obtained by performing one-way ANOVA analysis followed by the Tukey multiple comparisons test

A Small vessels (CD31⁺ cells)





**Fig. 4.**

Impaired intrathrombotic angiogenesis and recanalization and increased fibrotic remodeling in the ligated inferior vena cava (IVC) of *Akt2*^{-/-} mice. Wild-type (WT) mice and *Akt2*^{-/-} mice underwent a sham operation or IVC ligation. The thrombus-containing IVC was harvested at 2 weeks after ligation. **a** The IVC from WT or *Akt2*^{-/-} mice was stained with endothelial marker CD31. Intrathrombotic CD31-positive neovessels with tube-like formation were counted in 5 high-magnification fields ($\times 400$). Representative images of staining and quantification of the number of neovessels showing a significantly decreased number of neovessels in the ligated IVC of *Akt2*^{-/-} mice. All values represent the mean ($n = 6$ per group). P-values were obtained by performing one-way ANOVA analysis followed by the Tukey multiple comparisons test. **b** Representative images of immunofluorescence staining and quantification showing decreased vascular endothelial growth factor (VEGF) expression in the ligated IVC of *Akt2*^{-/-} mice. For the quantification of staining, the mean positive-staining area was normalized with the evaluated IVC area. All values represent the mean ($n = 6$ per group). P-values were obtained by performing multiple comparisons in one-way ANOVA analysis followed by the Tukey multiple comparisons test. **c** Representative images of immunofluorescence staining showing fibroblast specific protein (FSP)-1-positive cells in the ligated IVC of WT mice, which were even more abundant in the ligated IVC of *Akt2*^{-/-} mice. **d** Representative images of double immunofluorescence staining showing the colocalization of FSP-1 with the smooth muscle cell marker SM22- α in the vein wall and in the thrombus of ligated IVC in *Akt2*^{-/-} mice. **e, f** Representative images of immunofluorescence staining showing increased levels of **e** SMAD3 and **f** TGF- β in the ligated IVC of *Akt2*^{-/-} mice compared with WT mice

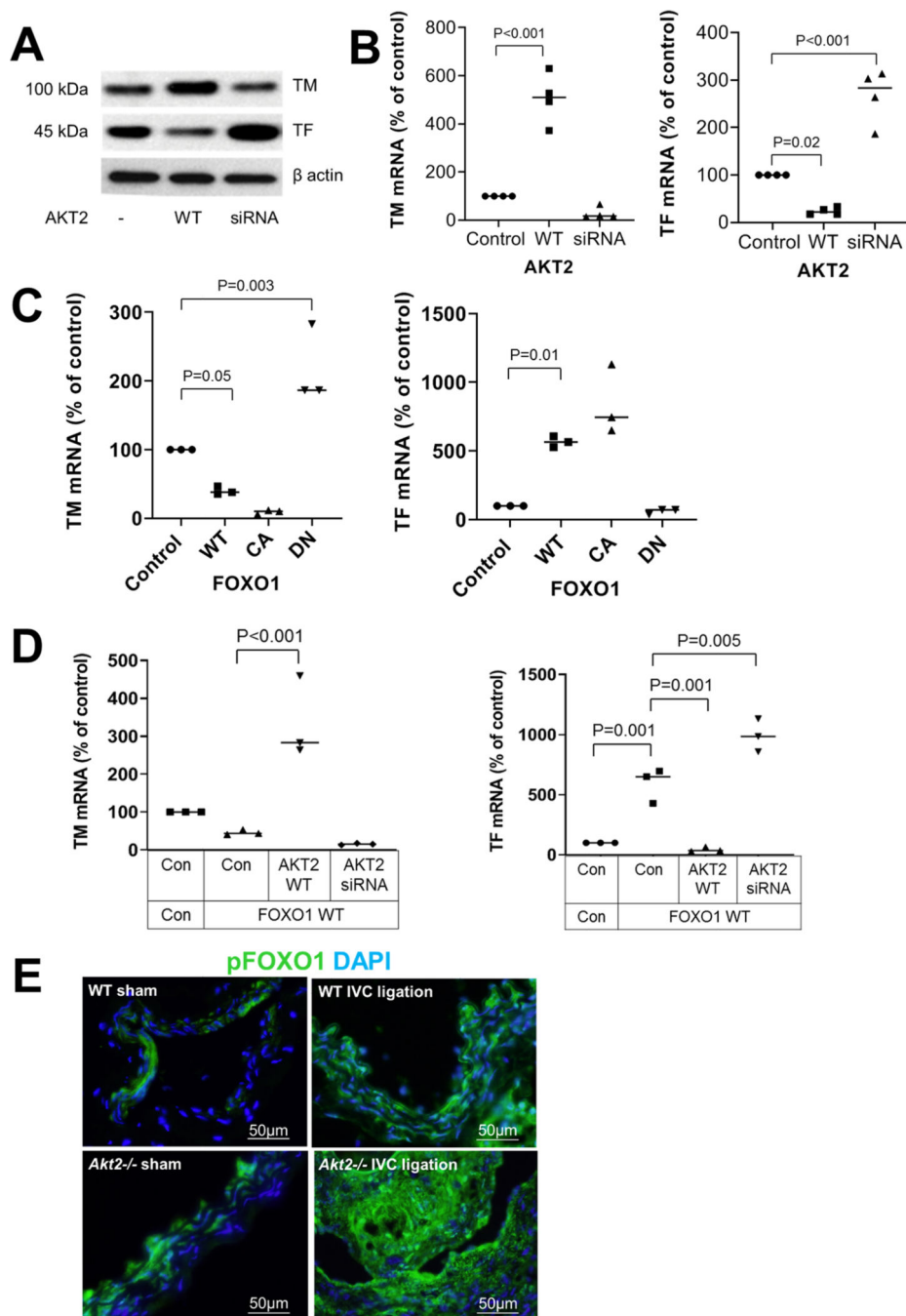


Fig. 5. Inhibition of the FOXO1-mediated regulation of thrombomodulin (TM) and tissue factor (TF) expression by AKT2. Human umbilical vein endothelial cells (HUVEC) were transfected with wild-type (WT)-AKT2 or AKT2 siRNA. Western blot analysis **a** and results of quantitative RT-PCR **b** showing a trend of induced TM expression and reduced TF expression by AKT2 overexpression. mRNA levels were normalized with those of β -actin and are expressed as the percentage of the control. Data represent the mean of 3 biologic repeats. **c** HUVECs were transfected with plasmids expressing WT-*FOXO1*, constitutively

active (CA)-*FOXO1*, or dominant negative (DN)-*FOXO1*. Quantitative RT-PCR results showing that WT-*FOXO1* and CA-*FOXO1* induced a trend of reduced TM expression and induced TF expression. DN-*FOXO1* had opposite effects. mRNA levels were normalized with those of β -actin and are expressed as the percentage of the control. Data represent the mean of 3 biologic repeats. **d** HUVECs were transfected with WT-*FOXO1* plasmid in the presence of WT-AKT2 and AKT2 siRNA. Quantitative RT-PCR results showing that AKT2 reversed the *FOXO1*-mediated inhibition of TM and stimulation of TF. The relative levels of mRNA are expressed as the percentage of the control. Data represent the mean of > 3 biologic repeats. P-values were obtained by performing multiple comparisons in one-way ANOVA analysis followed by the Tukey multiple comparisons test. **e** Wild-type (WT) mice and *Akt2*^{-/-} mice underwent a sham operation or IVC ligation. The thrombus-containing IVC was harvested at 2 weeks after ligation. Representative images of immunofluorescence staining showing increased phospho *FOXO1* (p-*FOXO1*) levels in the ligated IVC of *Akt2*^{-/-} mice compared with WT mice

Table 1

Antibodies used for immunostaining and Western blot experiments

Antibody	Vendor	Catalog number	Dilution
Immunostaining			
AKT2	Cell Signaling	4691	1:400
p-FOXO1	Thermo Fisher	PA5-104977	1:100
Thrombomodulin	Santa Cruz	SC-6192	1:50
Tissue factor	Santa Cruz	SC-374441	1:50
Endothelial protein C receptor (EPCR)	Santa Cruz	SC-28978	1:50
CD31	Santa Cruz	SC-376764	1:50
SM22a	Abcam	AB-89989	1:200
RIP3	Abcam	AB-68481	1:200
VEGF	Santa Cruz	SC-7269	1:50
FSP1	Santa Cruz	SC-73355	1:50
SMAD3	Santa Cruz	SC-8332	1:50
TGF	Santa Cruz	SC-146	1:50
Western blot			
Thrombomodulin	Santa Cruz	SC-9162	1:200
Tissue factor	Santa Cruz	SC-65962	1:200